Supplement of Atmos. Chem. Phys., 18, 10869–10879, 2018
https://doi.org/10.5194/acp-18-10869-2018-supplement

Atmospheric Chemistry and Physics
Open Access
EGU

Supplement of

Does afforestation deteriorate haze pollution in Beijing–Tianjin–Hebei (BTH), China?

Xin Long et al.

Correspondence to: Guohui Li (ligh@ieecas.cn)

Table S1 Land use categories in the MCD12Q1 IGBP layer and WRF-CHEM MODIS land use.

Land Cover Category	Category number	
	WRF-CHEM MODIS	**MOD12Q1**
Evergreen Needleleaf forest	1	1
Evergreen Broadleaf forest	2	2
Deciduous Needleleaf forest	3	3
Deciduous Broadleaf forest	4	4
Mixed forest	5	5
Closed shrublands	6	6
Open shrublands	7	7
Woody savannas	8	8
Savannas	9	9
Grasslands	10	10
Permanent wetlands	11	11
Croplands	12	12
Urban and built-up	13	13
Cropland/Natural vegetation mosaic	14	14
Snow and ice	15	15
Barren or sparsely vegetated	16	16
Water	17	0
Wooded Tundra	18	×
Mixed Tundra	19	×
Barren Tundra	20	×
Unclassified	×	254
Fill Value	×	255

Table S2 Threshold of the area fractional coverage of green vegetation, minimal and maximal SFz0 used in the coupled unified Noah land-surface model.

Category No.	Land Cover Category	G_T	$SFz0_{min}$	$SFz0_{max}$
1	Evergreen Needleleaf forest	0.70	50	50
2	Evergreen Broadleaf forest	0.95	50	50
3	Deciduous Needleleaf forest	0.70	50	50
4	Deciduous Broadleaf forest	0.80	50	50
5	Mixed forest	0.80	20	50
6	Closed shrublands	0.70	1	5
7	Open shrublands	0.70	1	6
8	Woody savannas	0.70	1	5
9	Savannas	0.50	15	15
10	Grasslands	0.80	10	12
11	Permanent wetlands	0.60	30	30
12	Croplands	0.80	5	15
13	Urban and built-up	0.10	50	50
14	Cropland/Natural vegetation mosaic	0.80	5	14
15	Snow and ice	0.00	0.1	0.1
16	Barren or sparsely vegetated	0.01	1	1
17	Water	0.00	0.01	0.01
18	Wooded Tundra	0.60	30	30
19	Mixed Tundra	0.60	15	15
20	Barren Tundra	0.30	5	10

Supplementary Figure Captions

Figure S1 Spatial distribution of (a) Organic carbon (OC), (b) Volatile organic compound (VOCs), (c) Nitrogen oxide, and (d) Sulfur dioxide (SO_2) emission rates in December 2013.

Figure S2 Comparison of the simulated (a) wind direction (wdir), (b) wind speed (wspd), and (c) planetary boundary layer height (PBLH) with the reanalysis data from ECMWF at monitoring sites in BTH from 1 December 2013 to 31 January 2014. The black dots represent the observations, and the red lines denote the reanalysis data. Data are averaged over all monitoring stations in BTH.

Figure S3 Pattern comparisons of simulated (color counters) vs. observed (colored circles) near-surface $PM_{2.5}$ mass concentrations averaged during each episode. The black arrows indicate simulated surface winds.

Figure S4 Horizontal distribution of near-surface $PM_{2.5}$ mass concentration changes caused by the afforestation during each episode. The wind field changes are shown in black arrows.

Figure S5 Horizontal distributions of aerosol species mass concentrations and changes due to the afforestation for (a1, a2) organic aerosol (OA), (b1, b2) sulfate (SO_4), (c1, c2) nitrate (NO_3), (d1, d2) ammonium (NH_4), and (e1, e2) elemental carbon (EC) during the episodes.

Figure S6 Horizontal distributions of (a) the average near surface BSOA mass concentration and (b) its change due to the afforestation during the episodes.

Figure S7 Horizontal distributions of (a) planetary boundary layer height (PBLH), (c) upward sensible heat flux (HFX) and (e) water vapor mixing ratio (QVAPOR), as well as (b, d, f) corresponding changes caused by the afforestation during the episodes, respectively.

Figure S8 Chinese vegetation regionalization. The BTH and ROI are highlighted with black lines. The data set is provided by Data Center for Resources and Environmental Sciences, Chinese Academy of Sciences (RESDC) (http://www.resdc.cn).

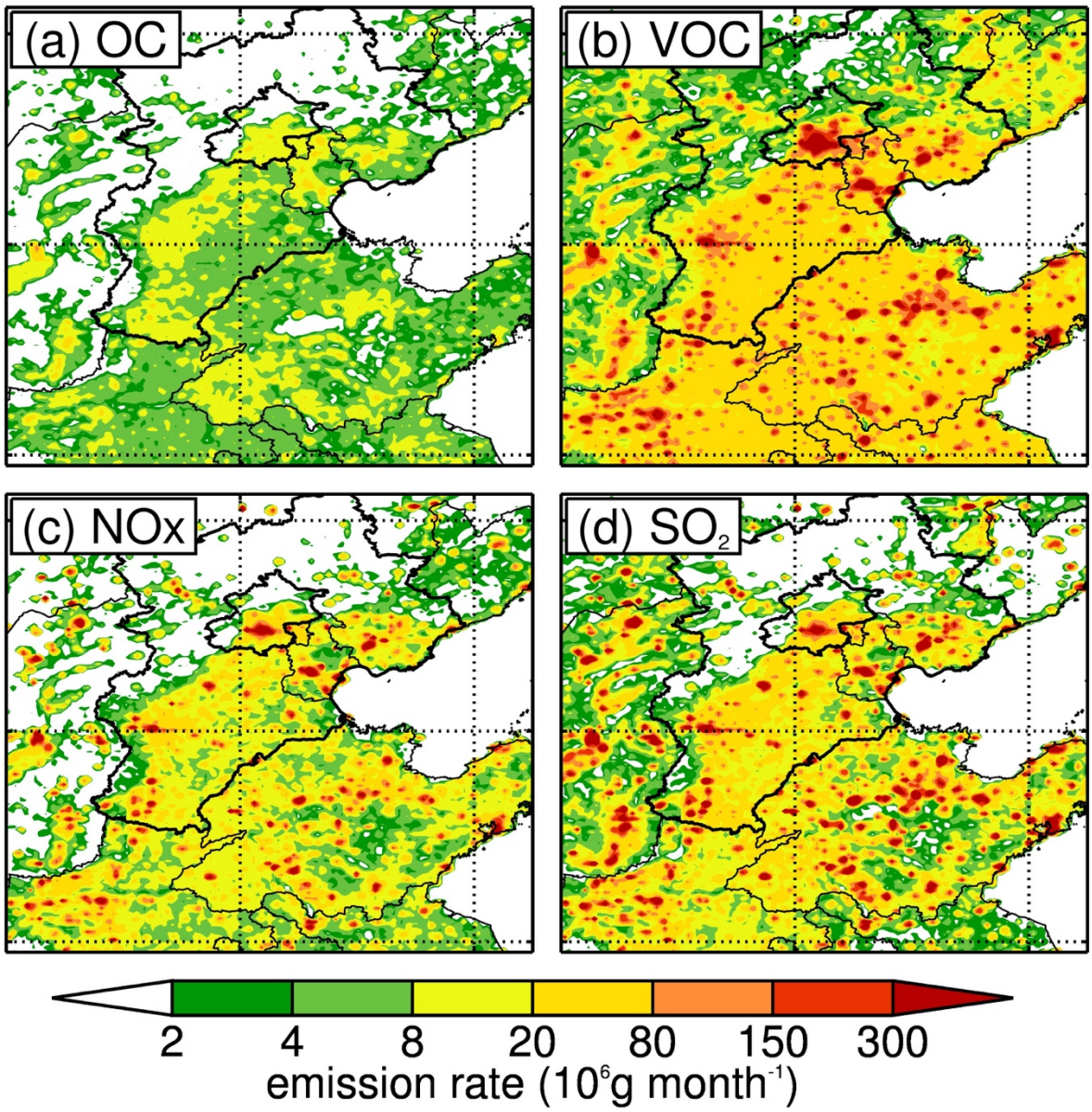

Figure S1 Spatial distribution of (a) Organic carbon (OC), (b) Volatile organic compound (VOCs), (c) Nitrogen oxide, and (d) Sulfur dioxide (SO_2) emission rates in December 2013.

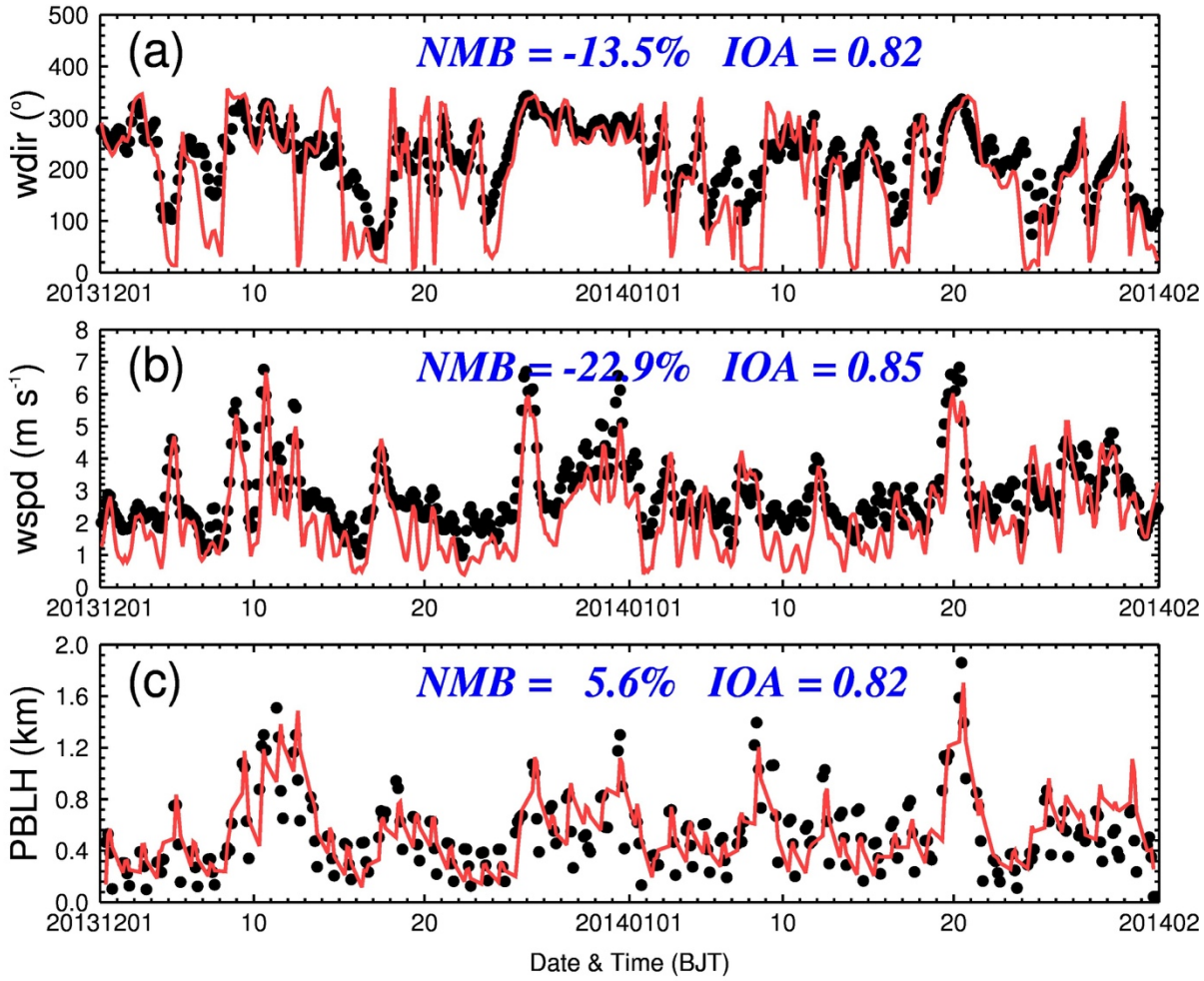

Figure S2 Comparison of the simulated (a) wind direction (wdir), (b) wind speed (wspd), and (c) planetary boundary layer height (PBLH) with the reanalysis data from ECMWF at monitoring sites in BTH from 1 December 2013 to 31 January 2014. The black dots represent the observations, and the red lines denote the reanalysis data. Data are averaged over all monitoring stations in BTH.

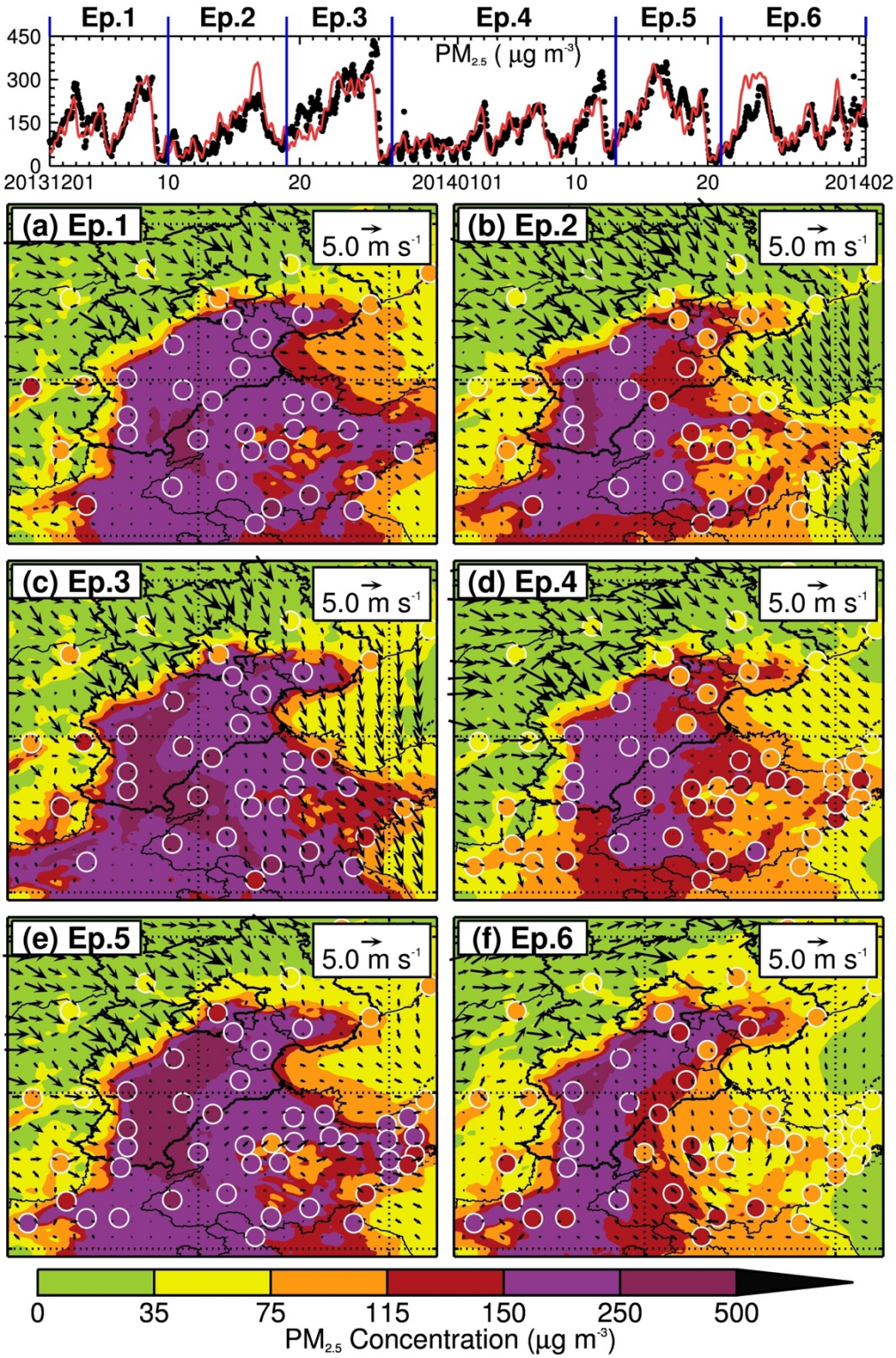

97
98
99 Figure S3 Pattern comparisons of simulated (color counters) vs. observed (colored circles)
100 near-surface $PM_{2.5}$ mass concentrations averaged during each episode. The black arrows
101 indicate simulated surface winds.
102
103
104

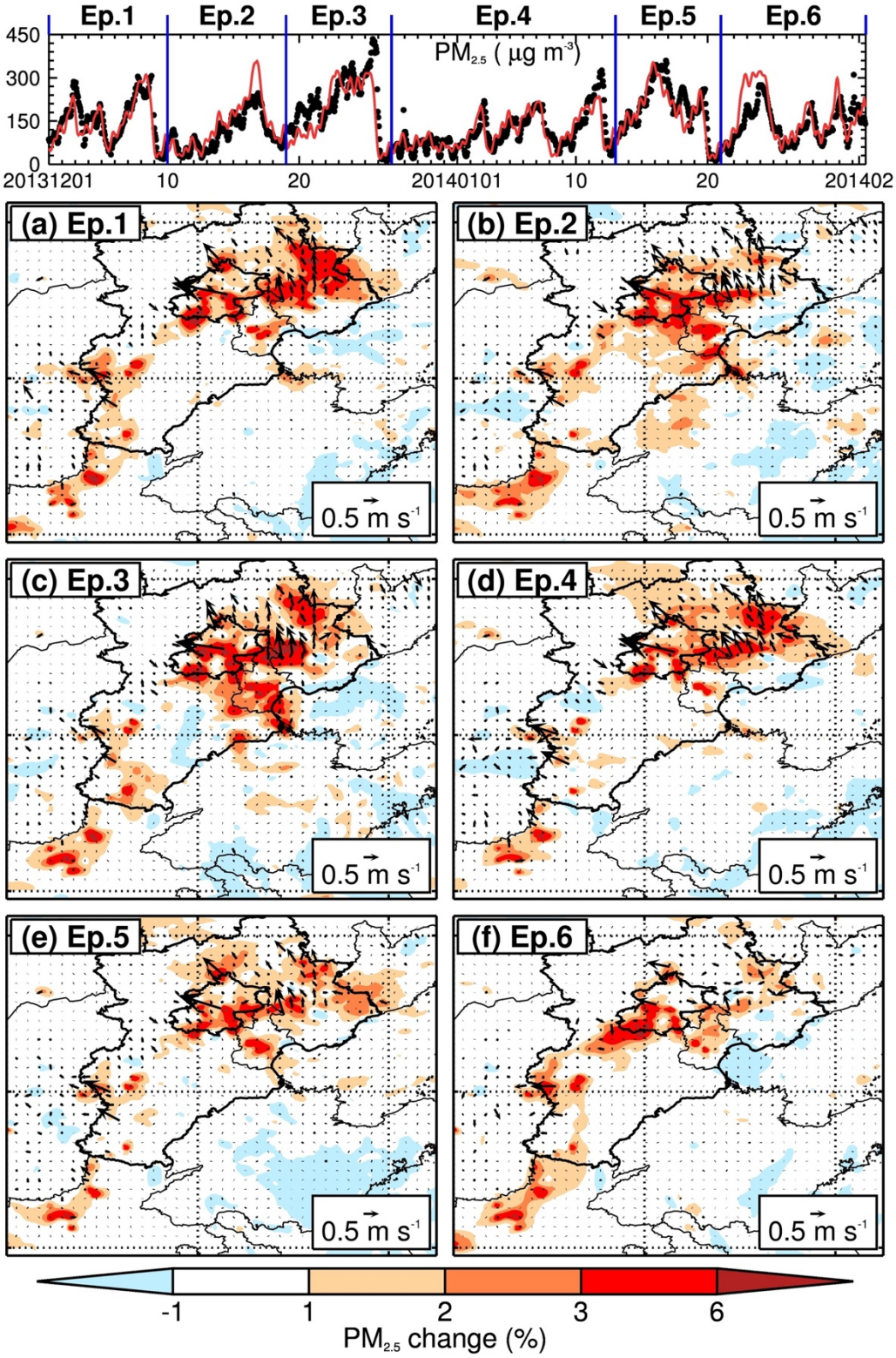

Figure S4 Horizontal distribution of near-surface $PM_{2.5}$ mass concentration changes caused by the afforestation during each episode. The wind field changes are shown in black arrows.

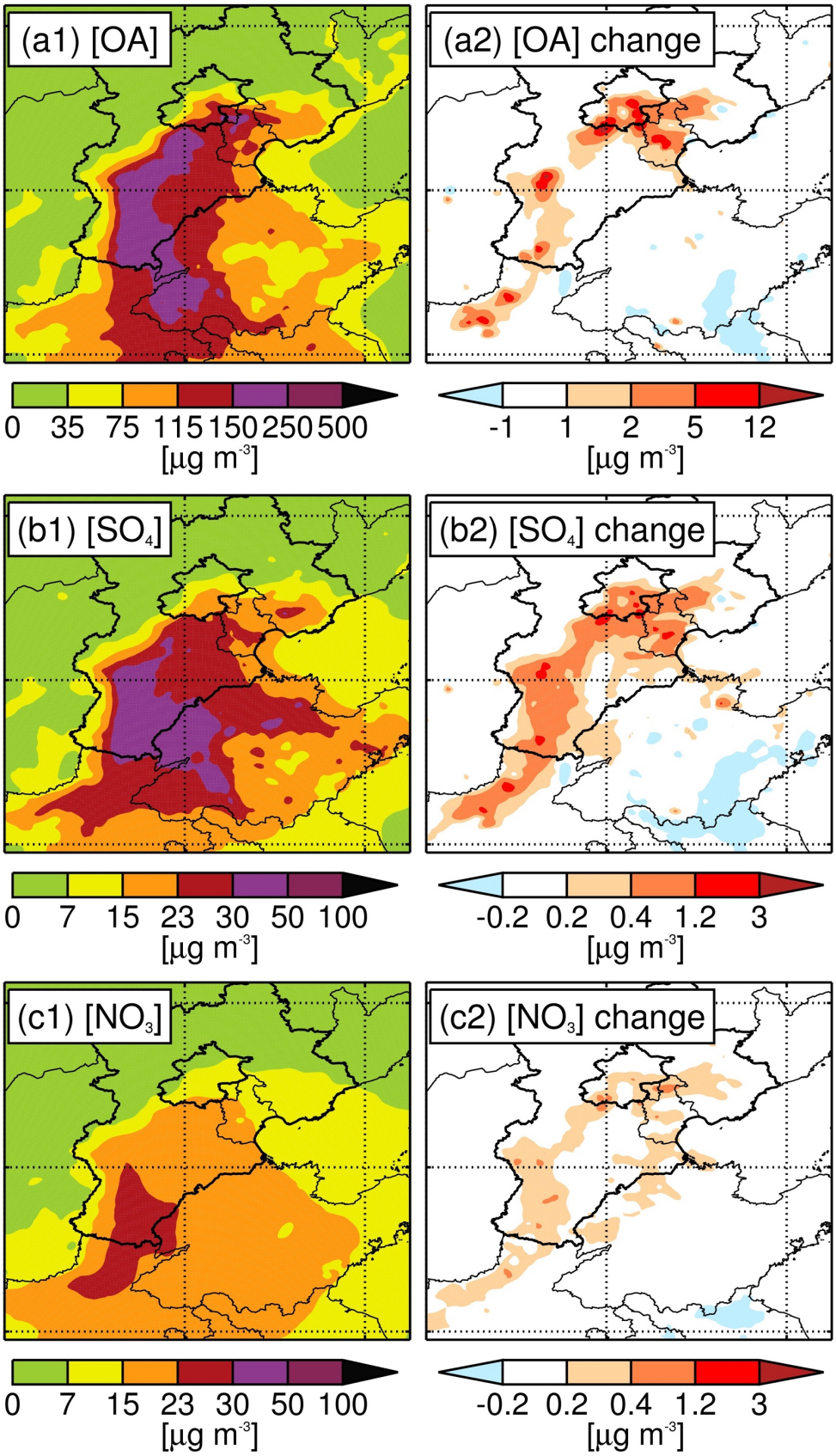

Figure S5 Horizontal distributions of aerosol species mass concentrations and changes due to the afforestation for (a1, a2) organic aerosol (OA), (b1, b2) sulfate (SO_4), (c1, c2) nitrate (NO_3), (d1, d2) ammonium (NH_4), and (e1, e2) elemental carbon (EC) during the episodes.

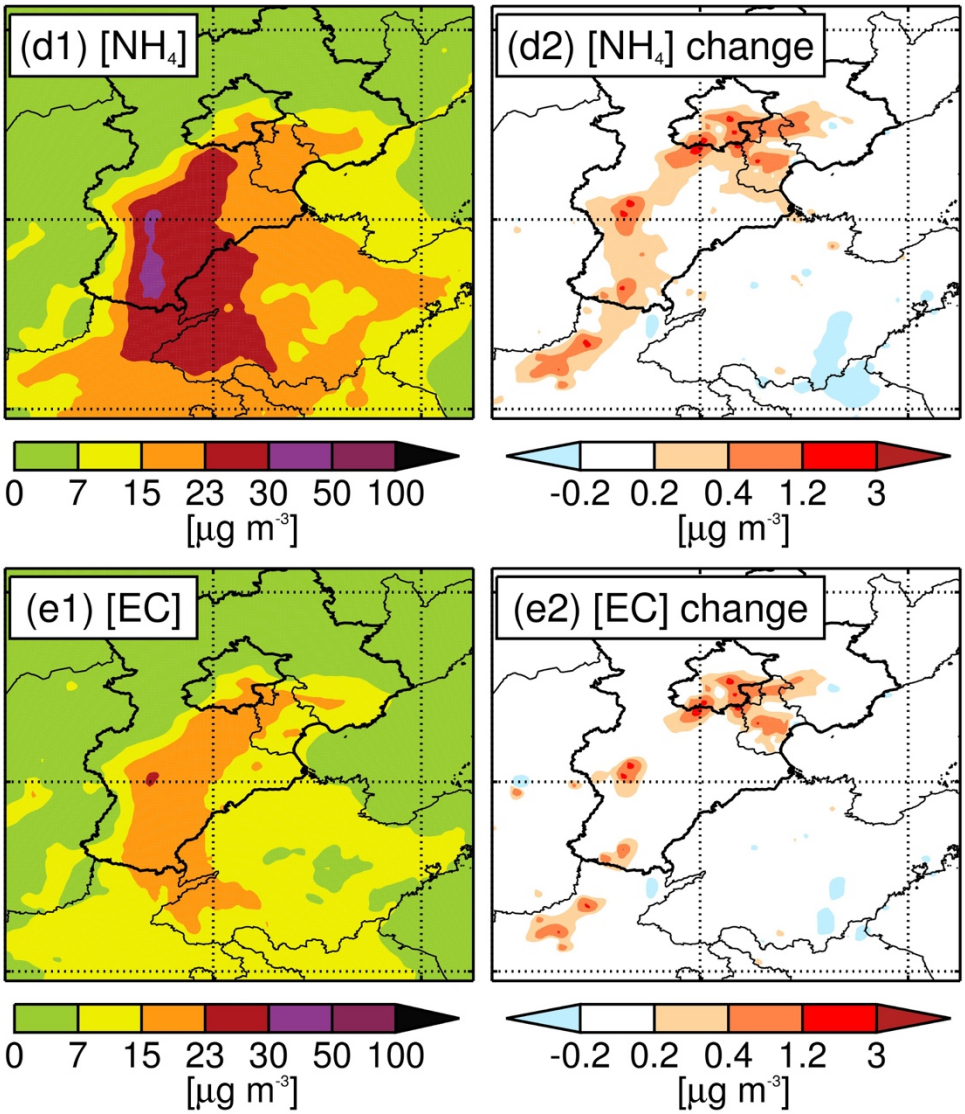

Figure S5 Continued

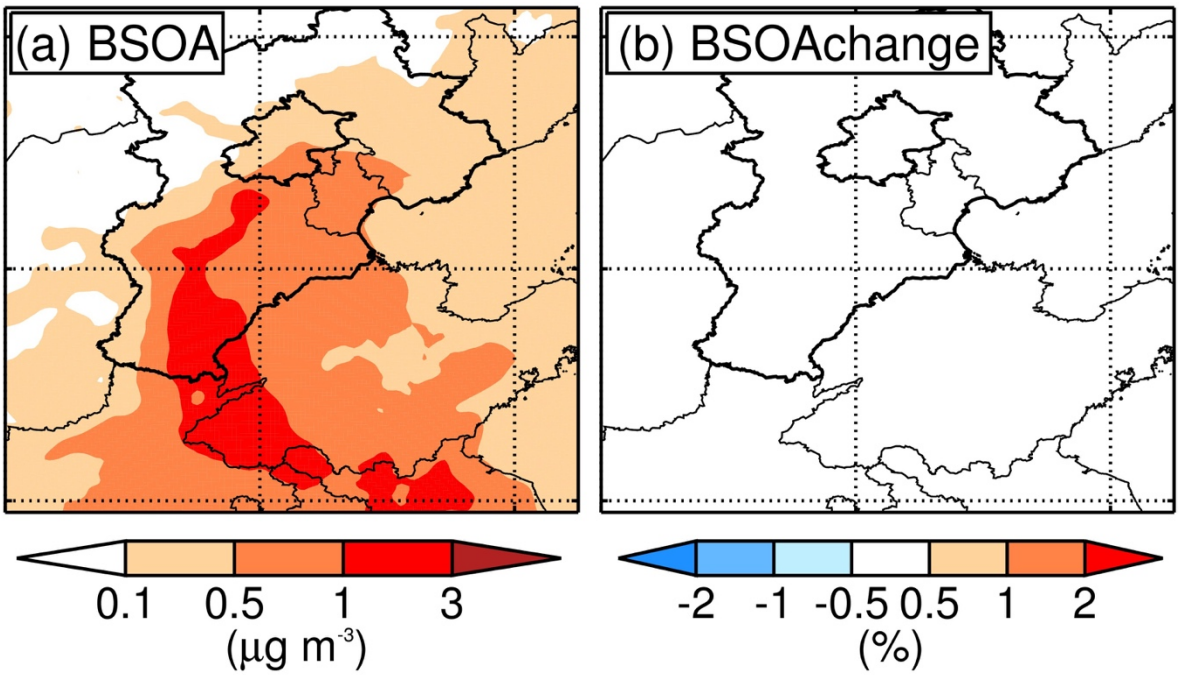

Figure S6 Horizontal distributions of (a) the average near surface BSOA mass concentration and (b) its change due to the afforestation during the episodes.

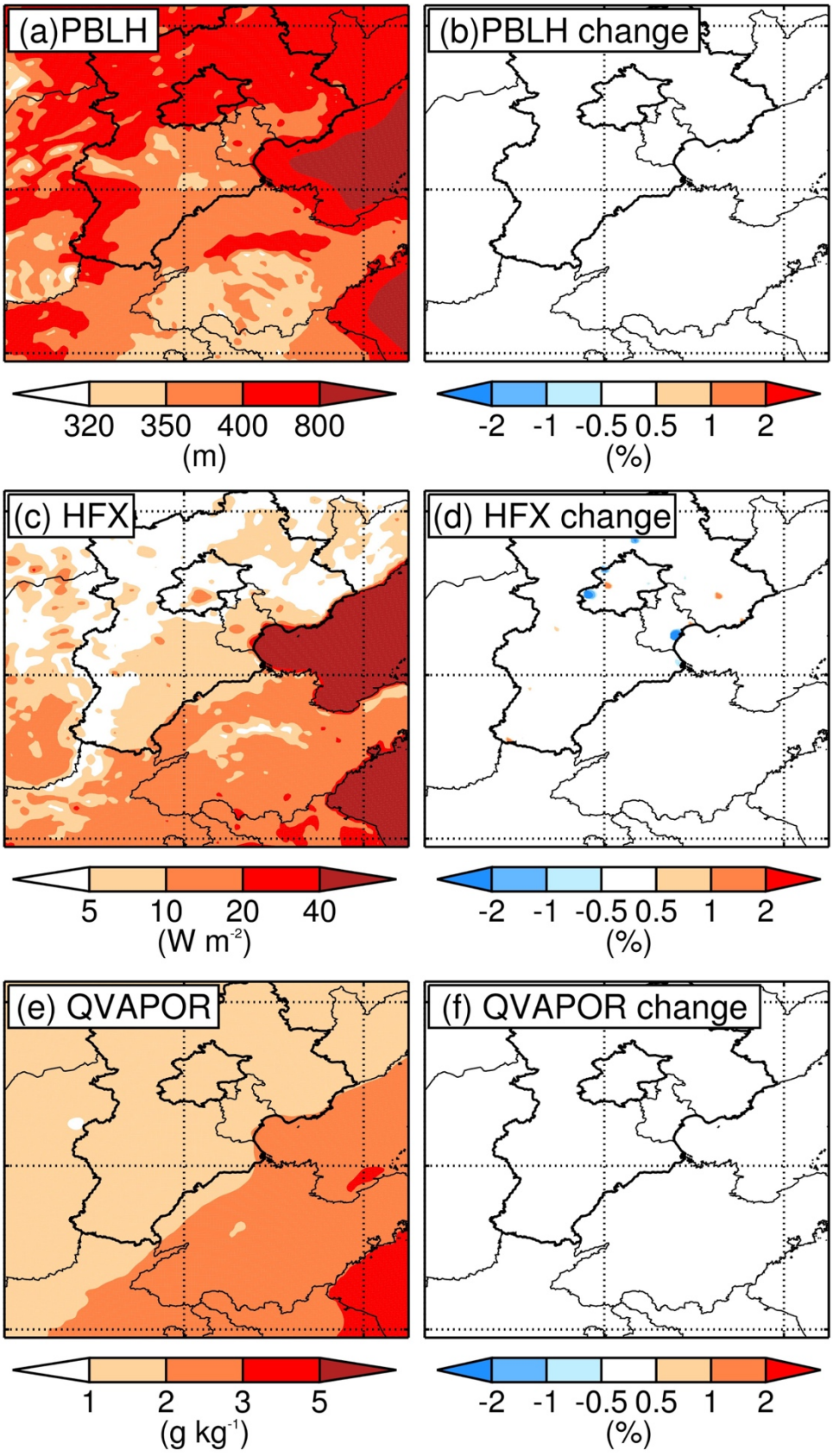

Figure S7 Horizontal distributions of (a) planetary boundary layer height (PBLH), (c) upward sensible heat flux (HFX) and (e) water vapor mixing ratio (QVAPOR), as well as (b, d, f) corresponding changes caused by the afforestation during the episodes, respectively.

Figure S10

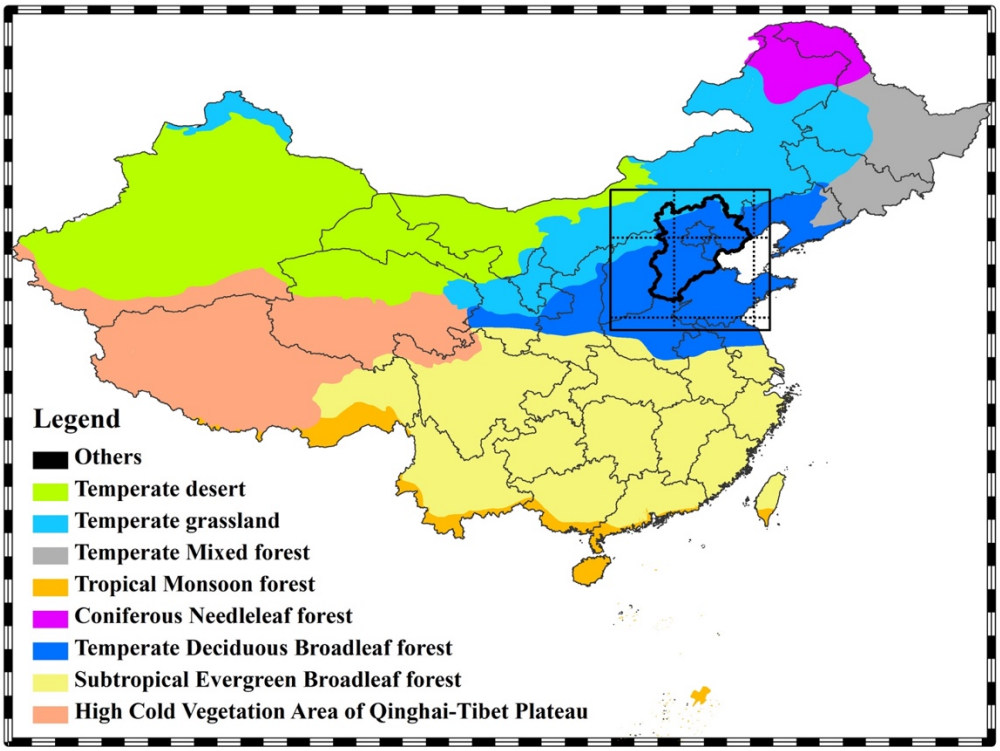

Figure S8 Chinese vegetation regionalization. The BTH and ROI are highlighted with black lines. The data set is provided by Data Center for Resources and Environmental Sciences, Chinese Academy of Sciences (RESDC) (http://www.resdc.cn).